SUPPLEMENTARY TEXT

Biochemical function of Pbx1 and Pbx2

A variety of enzymes that degrade glycans, such as pectin lyases, pectate lyases, and rhamnogalacturonases, contain parallel beta helix domains similar to the Pbx proteins (1). In environmental fungi, these enzymes enable the utilization of complex energy sources (2). Based on this, we tested the growth of wild type and *pbx* mutants on pectin, pectin galactan, polygalacturonic acid, rhamnogalacturonan, and xyloglucan, but detected no differences that would suggest a role for the Pbx proteins (not shown). We also considered the role of similar degradative enzymes in phytopathogenic fungi, where they act in plant cell wall degradation and the initation of infection (3). To pursue this idea, we assessed the growth of the *pbx* mutants on *A. thaliana* plant leaves, using a model similar to that used by Chaturvedi *et al.* for *C. neoformans* var. *gattii* (4). We were able to recover *C. neoformans* from plant leaves up to three weeks after infection, but observed no differences in colony forming units between mutant and wild type cells (data not shown).

In a further attempt to detect specific degradative activity of the Pbx proteins, we turned to *in vitro* assays, using both cell lysates from wild type and *pbx* mutants and recombinant GST-Pbx fusion proteins expressed and purified from *E. coli*. (For GST-fusion proteins, each complete Pbx coding sequence was cloned into the *Not1* and *Sma1* sites of pGEX-6P-1 from GE Life Sciences; proteins were purified by glutathione resin purification as per manufacturer recommendations.) We tested purified fusion proteins and cell lysates for their ability to degrade pectin, pectin galactan, polygalacturonic acid, rhamnogalacturonan, xylan, xyloglucan, chitin,and GXM,

assessing activity by detecting released products by thin layer chromatography (for hydrolases) or spectrometry (for lyase assays). Although we were able to demonstrate degradative activity of control enzymes, we were unable to detect any specific Pbx activity in these studies (not shown).

Cell wall degrading proteins in other fungi have been reported to influence the uptake, and thereby utilization, of simple sugars (5). Since *pbx* mutants grow better than wild type cells on xylose we tested their ability to incorporate radiolabeled xylose and glucose, but found no differences (data not shown). We also assayed recombinant Pbx proteins for two key activities of fungal xylose catabolism, xylose reductase and xylitol dehydrogenase, but were not able to demonstrate these biochemical activities. Finally, we tested Pbx protein binding to glycans, because CASH domains (Fig. S8) are characteristic of carbohydrate binding proteins (6)). The purified recombinant GST-Pbx fusion proteins did not interact with GXM in a surface Plasmon resonance assay (data not shown). Furthermore, screening them on a glycan array (Consortium for Functional Glycomics, array version 5.0) and testing biotinylated versions with potential partners by bio-layer interferometry did not identify specific binding partners (not shown).

To further characterize the *pbx*Δ mutants, we also compared their growth on various carbon sources. We detected a slight enhancement of mutant growth compared to wild type and complemented strains at 37 °C on glucose (Fig. S7, top row) or galactose (not shown); this was more pronounced on xylose, especially at higher temperatures (Fig. S7, bottom row).

References:

1. **Jenkins J, Mayans O, Pickersgill R.** 1998. Structure and evolution of parallel beta-helix proteins. J Struct Biol **122:**236-246.
2. **Mellon JE, Cotty PJ, Dowd MK.** 2007. *Aspergillus flavus* hydrolases: their roles in pathogenesis and substrate utilization. Appl Microbiol Biotechnol **77:**497-504.
3. **Lagaert S, Belien T, Volckaert G.** 2009. Plant cell walls: Protecting the barrier from degradation by microbial enzymes. Semin Cell Dev Biol **20:**1064-1073.
4. **Springer DJ, Ren P, Raina R, Dong Y, Behr MJ, McEwen BF, Bowser SS, Samsonoff WA, Chaturvedi S, Chaturvedi V.** 2010. Extracellular fibrils of pathogenic yeast *Cryptococcus gattii* are important for ecological niche, murine virulence and human neutrophil interactions. PLoS One **5:**e10978.
5. **Tonukari NJ, Scott-Craig JS, Walton JD.** 2000. The *Cochliobolus carbonum SNF1* gene is required for cell wall-degrading enzyme expression and virulence on maize. Plant Cell **12:**237-248.
6. **Ciccarelli FD, Copley RR, Doerks T, Russell RB, Bork P.** 2002. CASH--a beta-helix domain widespread among carbohydrate-binding proteins. Trends Biochem Sci **27:**59-62.

SUPPLEMENTARY TABLES

Supplemental Table 1.

Primers used in this study. Underlined sequences are complementary to genome sequence, and lower case text denotes restriction sites.

PK-001	CCGCCAATAGAGCACCGATG
PK-002	GCTTGATATCGAATTCCTGCAGCCCGGGACGATGAAGAACACCGATG
PK-003	CGGGCTGCAGGAATTCGATATCAAGC
PK-004	CCACTCTTGACGACACGGCTTACC
PK-005	GCTCATGTAGAGCGCCTGCTC
PK-006	GCTGCGAGGATGTGAGCTGG
PK-007	GCTCTCCAGCTCACATCCTCGCAGCGCATCGTAGCAGCAGGTATCC
PK-008	CCTACAGTGCGGTGCAGATTC
PK-009	CCTATCCTAGTCGTCAGCACC
PK-010	GCCGACTTCTTCCCTAACACC
PK-011	GCACGGCTCAATGCGAATGA
PK-012	CGACGCGCTTGTAAGGATCAG
PK-013	GCAACGCCGTTGAATCCTCAG
PK-014	CCTCCGACAACCATACACTCAG
PK-015	CATCGCTTCCGATTACACTCC
PK-016	CACCCTCTTGTCGGATATCATCTGTCCCCTGATCGCCAGATACGAGG
PK-017	GGACAGATGATATCCGACAAGAGG
PK-018	CCTGAATGAACTGCAGGACG
PK-019	GCCAACGCTATGTCCTGATAGC
PK-020	GCTCTCCAGCTCACATCCTCGCAGCCCACTCCGGAGGAGTCTAAAG
PK-021	GCCATGTCAAGTGCAGAACAG
PK-022	GAGCCATGCGTCATGTGTTGG
PK-023	CCTTCCATCAACAGATGGCG
PK-024	GGATCGCAGTCAGCATTGTG
PK-025	CTCGCCTCCTATGGAACATAGC
PK-026	CGCTCTCTGTACCATGCTTGTG
PK-201	GTAAACTCGCCCAACcacgtgATGCCTTGGCCCTCGGTG
PK-202	CATCGTAAGGGTAAGcgccggcgCCAGACCATTTATTGCTCCTAGCC
PK-203	GTAAACTCGCCCAACcacgtgATGGCTGTCAGCCCTCTAC
PK-204	CGTAAGGGTAAGcgccggcgCCCAGAAGCTTCCCATGGAC
MSPC-114	AACGCTGCGAGGATGTGAGCTGGA
MSPC-115	GACTTGTCGAGTCGAGACATCACGTGGTTGGGCGAGTTTACTAATGGA
MSPC-116	CGTGATGTCTCGACTCGACAAGTCCCTAGGTTCGTGAAGGCGGTAAGG

MSPC-117 TCATCGATGAAGAGTGTGCAGGCAAAGGT

Supplemental Table 2.

NMR assignment of proton and carbon peaks of mannosyl triad M2

Residue		Chemical shifts in ppm							
		1	2	3	4	5_{ax}	5_{eq}	6	6'
α-Man^{A}	^{1}H	5.25	4.28	4.05	3.87	3.96		3.79	3.87
	^{13}C	103.1	80.1	80.3	69.1	76.1		63.2	
α-Man^{B}	^{1}H	5.30	4.22	4.07	3.80	3.96		3.79	3.87
	^{13}C	103.1	81.0	79.1	69.3	76.1		63.2	
α-Man^{C}	^{1}H	5.18	4.23	4.07	3.72	3.98		3.79	3.87
	^{13}C	104.0	80.1	78.9	69.8	76.1		63.2	
β-GlcA^{A}	^{1}H	4.49	3.39	3.50	3.60	3.74			
	^{13}C	104.5	75.2	78.2	74.2	78.9		177.0	
β-Xyl^{B}	^{1}H	4.49	3.30	3.45	3.64	3.31	4.00		
	^{13}C	105.9	75.6	78.4	72.1	67.9			
β-Xyl^{C}	^{1}H	4.39	3.32	3.43	3.64	3.27	4.01		
	^{13}C	106.1	75.6	78.4	72.1	67.9			

Supplemental Table 3.

NMR assignment of proton and carbon peaks of mannosyl triad M3.

Residue		Chemical shifts in ppm							
		1	2	3	4	5_{ax}	5_{eq}	6	6'
α-Man^{A}	^{1}H	5.204	4.26	4.20	4.02	4.05		3.95	3.95
	^{13}C	102.4	79.9	77.0	78.0	75.5		62.5	
α-Man^{B}	^{1}H	5.30	4.19	4.06	3.86	3.88		3.85	3.85
	^{13}C	102.8	80.8	78.9	69.1	76.1		63.0	
α-Man^{C}	^{1}H	5.144	4.15	4.04	3.69	3.93		3.79	3.87
	^{13}C	103.3	80.3	78.0	70.0	76.1		63.4	
β-GlcA^{A}	^{1}H	4.49	3.40	3.49	3.61	3.72			
	^{13}C	104.2	75.2	78.4	74.2	78.9		177.0	
β-Xyl^{A}	^{1}H	4.41	3.28	3.45	3.58	3.33	3.88		
	^{13}C	106.6	76.6	78.9	72.4	67.7			
β-Xyl^{B}	^{1}H	4.49	3.31	3.45	3.64	3.29	4.00		
	^{13}C	106.1	75.6	78.4	71.9	67.7			
β-Xyl^{C}	^{1}H	4.27	3.35	3.41	3.68	3.18	4.08		
	^{13}C	105.6	75.6	78.4	71.9	68.1			

Supplemental Table 4.

Chemical shift assignments of 2-O-acetylated mannose and attached xylose residues in GXMGal from *cap59* cells.

No.	Residue		Chemical shift							NOE
			1	2	3	4	5	6	6'	HMBC
I	3-(2-OAc)-α-Man	^{1}H	5.24	5.36	4.21	3.84	3.95	3.83	3.73	2,3-Man H-3
		^{13}C	101.6	71.7	78.3	67.8	75.9	63.1		2,3-Man C-3
II	β-Xyl	^{1}H	4.49	3.28	3.45	3.63	3.99	3.33		1-2,3
		^{13}C	103.1	75.4	78.3	72.0	67.9			1-3

66

SUPPLEMENTARY FIGURES

Supplemental Fig. S1.

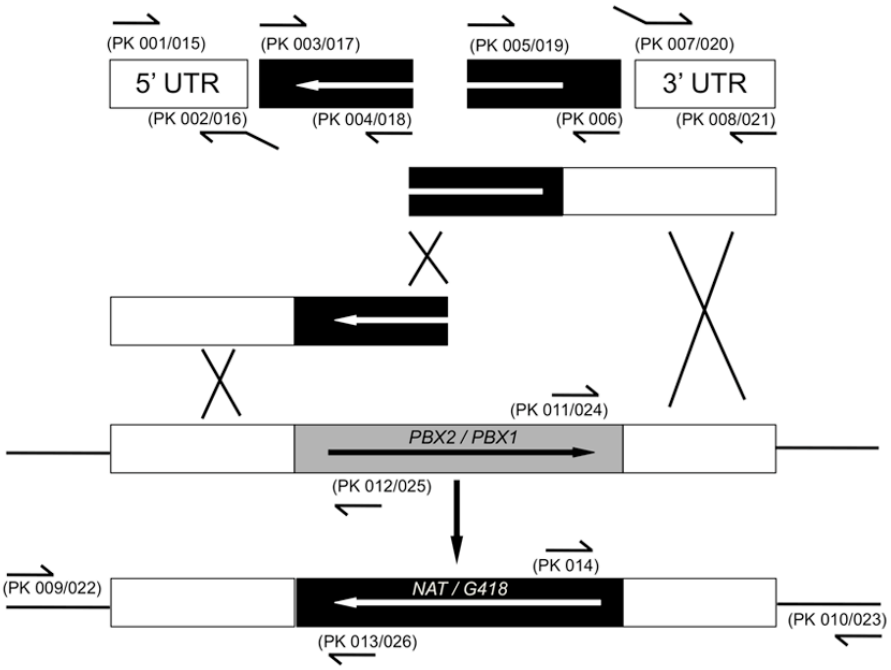

Fig. S1. The split marker strategy used to generate *pbx*Δ strains. The positions of primers used to generate fragments for *PBX2/PBX1* deletion and to screen for gene replacement are shown. See Methods for details and Supplemental Table 1 for primer sequences. Drawing is not to scale.

Supplemental Fig. S2.

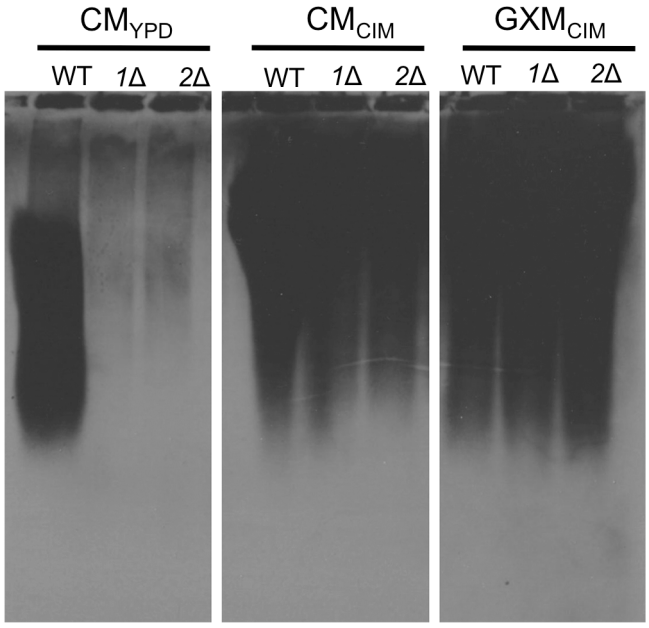

Fig. S2. Immunoblot analysis of CM or purified GXM from the indicated strains, grown in rich (YPD) or capsule-inducing (CIM) medium. Samples (50 µl of CM or 10 µg of GXM) were resolved by agarose gel electrophoresis and immunoblotted with antibody 3C2. A 5 minute exposure is shown to demonstrate the presence of low amounts of antibody reactive material in the CM from deletion strains grown in YPD. Compare to Fig. 2 in the main text (2 sec exposure).

Supplemental Fig. S3.

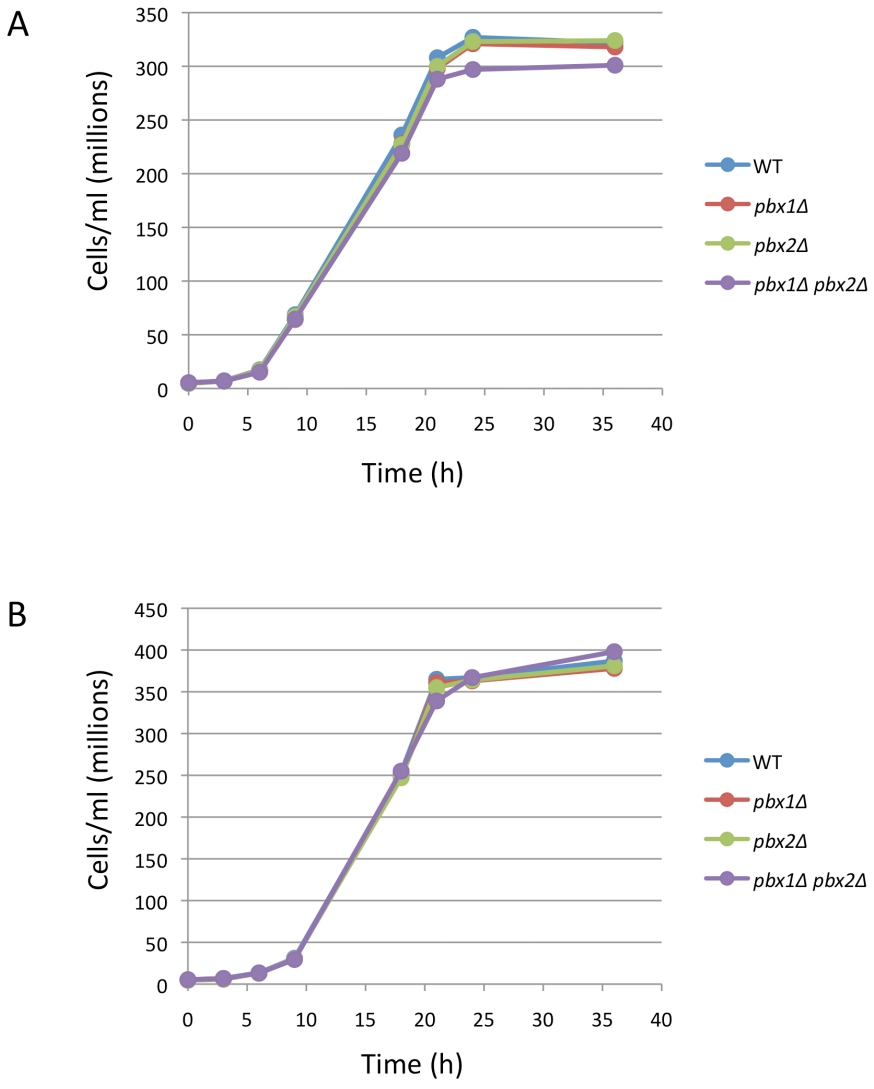

Fig. S3. *pbx*Δ mutants grow at the same rate as wild type in rich and capsule-inducing liquid medium. Cells were grown at 30 ºC with shaking in YPD (Panel A) or CIM (Panel; B), and counted periodically as described in the Methods. Growth rates are comparable for all strains although the final culture density of the double mutant is slightly below that of wild type and the single mutants in rich medium.

Supplemental Fig. S4.

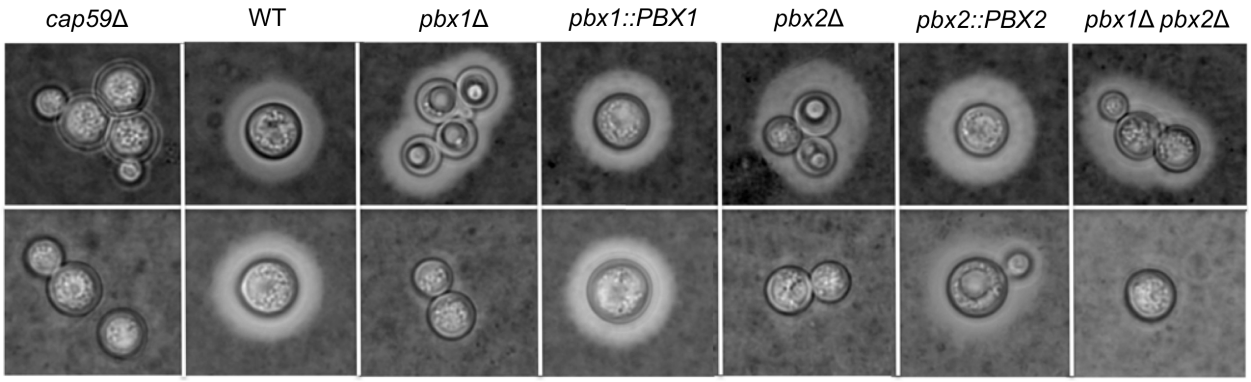

Fig. S4. The capsule of *pbx*Δ mutants responds to inducing conditions and is loosely associated with the cell wall. The indicated strains were grown in capsule-inducing medium for 36 h and stained with India ink before (top row) or after (bottom row) sonication. See Methods for details.

Supplemental Fig. S5.

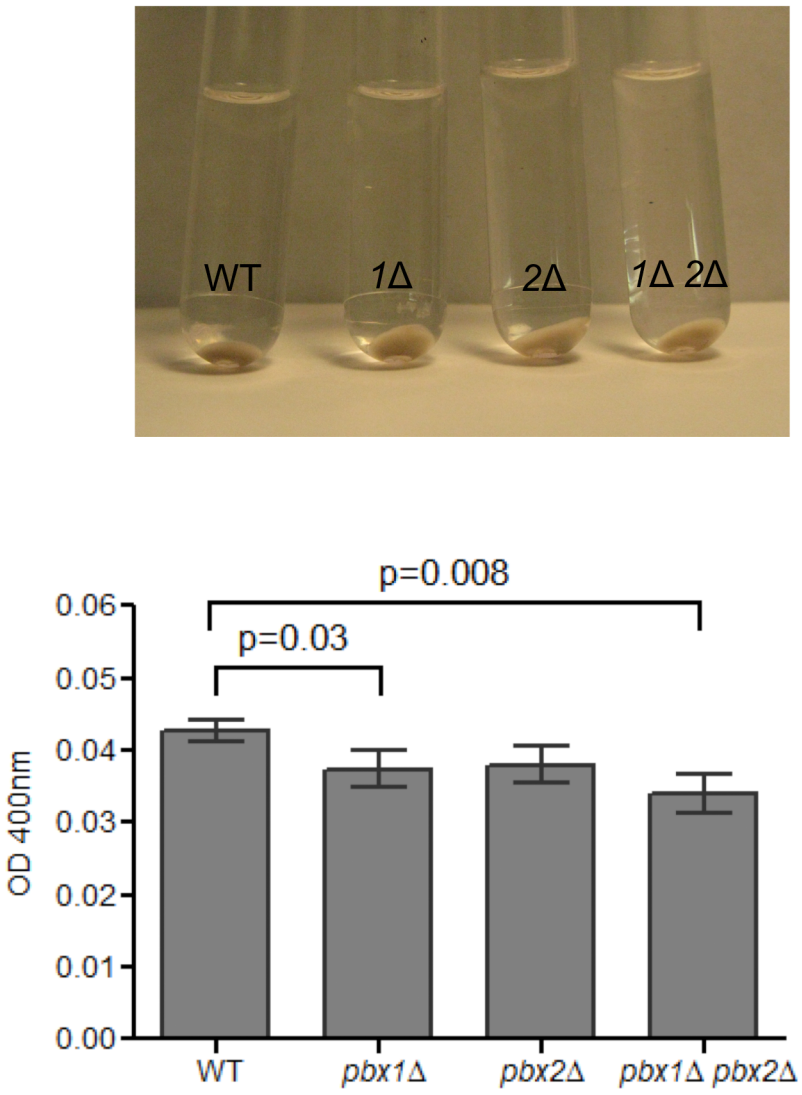

Fig. S5. *pbx*Δ mutants show a subtle reduction in melanin production, seen as slightly lighter cell pellets (top panel) and modestly reduced melanin release into the medium (bottom panel). Significant differences ($p < 0.05$ by t-test) are indicated by brackets.

Supplemental Fig. S6.

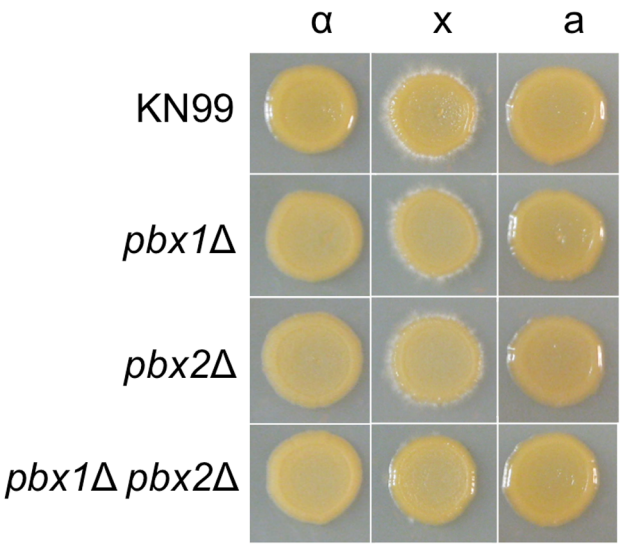

Fig. S6. The *pbx1*Δ *pbx2*Δ double mutant is defective in mating. Each *MAT*α strain indicated at the left was mixed with an equal number of KN99 *MAT***a** cells, spotted on V8 mating agar, and incubated in the dark for 2 weeks. The middle column shows the cross, while the flanking columns show the growth of each crossed strain alone. The top three crosses filamented normally, while very few filaments were seen with the cross of the double mutant strain.

Supplemental Fig. S7.

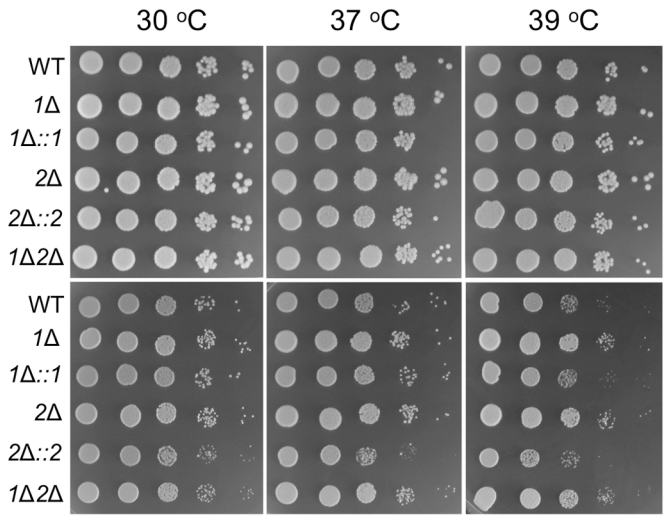

Fig. S7. *pbx*Δ mutants show a subtle enhancement of growth on glucose medium (top panels) at 37 °C, which becomes more pronounced on xylose (bottom panels), especially at higher temperatures. Serial 10-fold dilutions of the indicated strains were spotted on minimal medium with 2% glucose (top) or xylose (bottom) and incubated at the indicated temperatures for four days.

Supplemental Fig. S8.

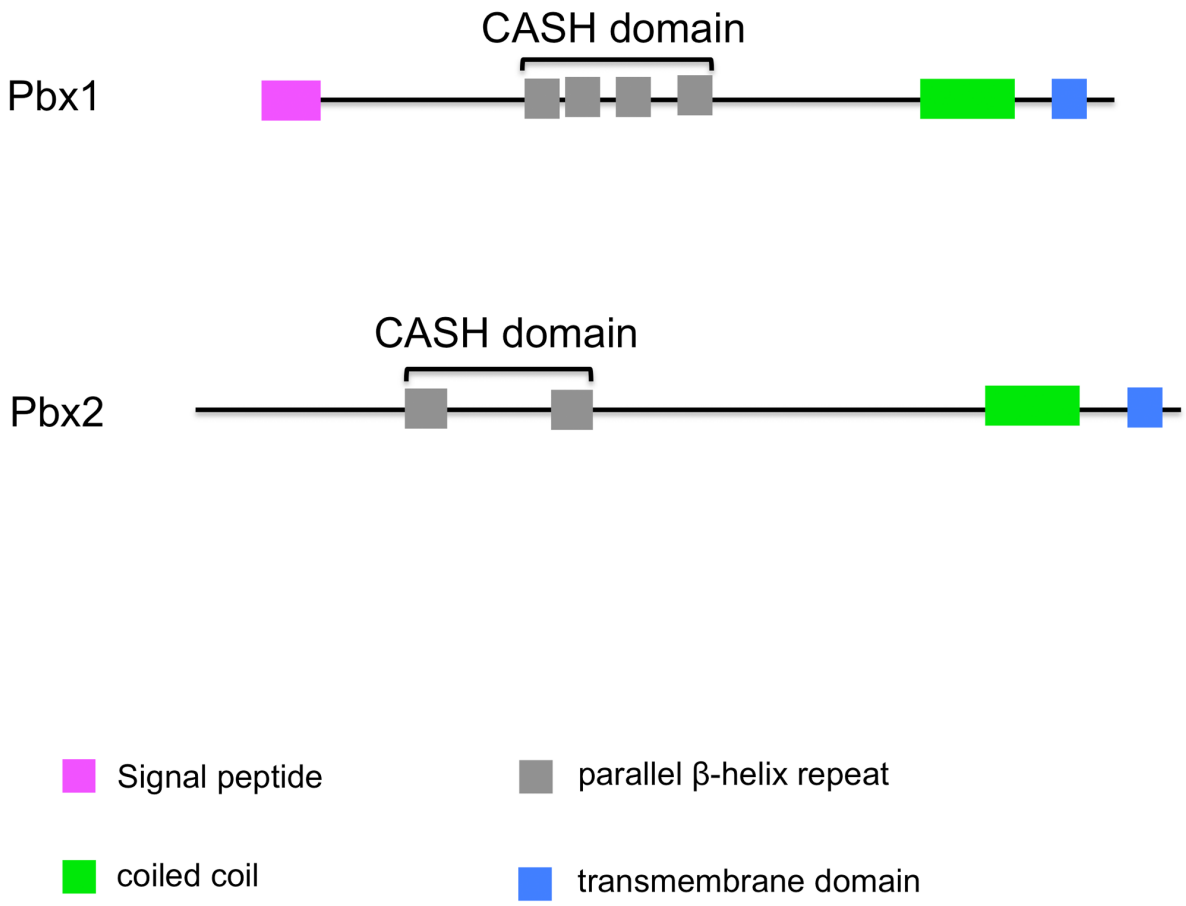

Fig. S8. Domain prediction of Pbx proteins based on a Simple Modular Architecture Research Tool (SMART; http://smart.embl-heidelberg.de/) search of their amino acid sequences. Both Pbx1 and Pbx2 are predicted to have carbohydrate binding and sugar hydrolase (CASH) domains.